Nitrate reduction by iron supported bimetallic catalyst in low and high nitrogen regimes

Shanawar Hamid and Woojin Lee[*]

Department of Civil and Environmental Engineering, Korea Advanced Institute of Science and Technology, 291 Daehak-ro, Yuseong-gu, Daejeon 34141, Republic of Korea

Abstract.   In this study, the effect of initial nitrate loading on nitrate removal and byproduct selectivity was evaluated in a continuous system. Nitrate removal decreased from 100% to 25% with the increase in nitrate loading from 10 to 300 mg/L NO_3-N. Ammonium selectivity decreased and nitrite selectivity increased, while nitrogen selectivity showed a peak shape in the same range of nitrate loading. The nitrate removal was enhanced at low catalyst to nitrate ratios and 100% nitrate removal was achieved at catalyst to nitrate ratio of $\geq$ 33 mg catalyst / mg NO_3-N. Maximum nitrogen selectivity (47%) was observed at 66 mg catalyst / mg NO_3-N, showing that continuous Cu-Pd-NZVI system has a maximum removal capacity of 37 mg NO_3^--N/$g_{catalyst}$ /h. The results from this study emphasize that nitrate reduction in a bimetallic catalytic system could be sensitive to changes in optimized regimes.

Keywords: Cu-Pd bimetallic catalyst; catalytic nitrate reduction; NZVI; reduction capacity; continuous system

1. Introduction

Recently, nitrate (NO_3^-) pollution in environment has increased due to industrial, agricultural, and domestic discharges. NO_3^- pollution to water bodies is most serious due to its potential hazards on human health and ecological cycle (Jung *et al*. 2014, Choi *et al*. 2012, Pirkanniemi and Sillanpaab 2002). The catalytic removal by supported bimetallic catalyst has emerged as promising technology to cope with enormous challenge of global NO_3^- pollution (Pinter 2003, Shin *et al*. 2014). In recent studies, it was reported that supported bimetallic catalyst can remove NO_3^- at high kinetic rates and good nitrogen (N_2) selectivity at optimized conditions (Hamid *et al*. 2015, Jung *et al*. 2012, 2014, Bae *et al*. 2013, Liou *et al*. 2009). However, NO_3^- concentration may vary with respect to source of NO_3^- disposal. For example, NO_3^- effluent from domestic disposal may be far less than that from agricultural or industrial waste waters. This means that unpredictable variation in NO_3^- loading in water stream/samples could be expected. In such scenarios, however, the catalytic removal process designed at specific optimized conditions may not stand to deliver expected removal efficiency and byproducts selectivity. Moreover, the nitrate removal capacity and byproduct selectivity could be sensitive to any change in catalyst to nitrogen

---

*Corresponding author, Professor, E-mail: woojin_lee@kaist.edu

ratios. Hence, more investigation is essential to evaluate the behavior of bimetallic catalyst at different NO_3^- loading regimes. In this study, NZVI was selected as support material due to its environmentally benign nature, high reactivity, inexpensive raw materials, and ease of synthesis (Liu *et al*. 2014, Hamid *et al*. 2015). Cu-Pd pair was selected as bimetallic combination due to its established high NO_3^- removal and N_2 selectivity (Jung *et al*. 2014, Choi *et al*. 2012, Soares *et al*. 2012, Al Bahari *et al*. 2013). The catalyst was evaluated for NO_3^- removal in continuous mode. The specific objectives of this study were 1) to characterize the catalyst by X-ray diffraction (XRD), transmission electron microscopy (TEM) and energy dispersive X-ray (EDX); 2) and to evaluate the effect of different NO_3^- loadings and catalyst ratios on NO_3^- removal and byproduct selectivity by Cu-Pd-NZVI catalyst.

2. Materials and methods

2.1 Chemicals

NZVI was prepared by Ferric chloride hexahydrate (98%, SigmaAldrich Inc., USA) and sodium borohydride (98.0%, Samchun Pure Chemical Co., Korea), as described elsewhere (Hamid *et al*. 2015). Copper(II) chloride dihydrate (97.5%, Samchun Pure Chemical Co., Korea) was used as Cu precursor and disodium tetrachloropalladate (98% Sigma-Aldrich Inc., USA) as Pd precursor. Potassium nitrate (99.0%, Duksan Pure Chemical Co., Korea) was used to prepare nitrate stock solution. Potassium nitrite (97.0%, Samchun Pure Chemical Co., Korea), and ammonium chloride (98.5%, Duksan Pure Chemical Co., Korea) were used to prepare standard solutions of nitrite and ammonium for ion chromatography (IC). Sodium bicarbonate (99.7%, Sigma-Aldrich Inc., USA), sodium carbonate (99.5%, Sigma-Aldrich Inc., USA), and nitric acid (60%) were used to prepare eluent for nitrite, nitrate, and ammonium measurement, respectively. Ultrapure water system (ELGA PURELAB Classic system) were used for deionized water, which was further purged with argon gas for 12 h to prepare deaerated deionized water (DDIW) (Hamid *et al*. 2015).

2.2 Catalyst preparation

NZVI was synthesized as described elsewhere (Hamid *et al*. 2015). To prepare NZVI support, 0.9 M $NaBH_4$ solution was added dropwise to a 0.11 M $FeCl_3 \cdot 6H_2O$ solution at continuous mixing and room temperature. NZVI thus prepared was vacuum filtered and washed with DDIW using a membrane filter (0.2 μm, Advantech, Japan). All the procedures were performed in anaerobic chamber to avoid oxidation. The newly synthesized NZVI was re-suspended in DDIW followed by sequential addition of Cu and Pd precursors and constantly mixed for 30 min each to prepare 0.5% Pd-1.5% Cu-NZVI (Cu-Pd-NZVI) catalyst. The Cu-Pd-NZVI catalyst was filtered in anaerobic chamber as described above, followed by drying at −81°C for 24 h in a freeze-dryer (Labconoco Freezone 6 plus, USA). The finally prepared catalyst was crimp capped in 5% H_2 and 95% N_2 media and then stored in the anaerobic chamber for further use.

2.3 Reactor

The experiments were conducted in a 500 mL glass reactor (200 mL effective volume for the catalytic test) as described in our recent study (Hamid *et al*. 2015). The conditions were fixed as

following: hydraulic retention time (HRT): 60 min; Hydrogen (H_2) gas: 30 mL/min; mixing speed: 300 rpm. After 30 min of H_2 purging, the required amount of catalyst was added to the reactor. Samples were collected and filtered by syringe filter (0.2 μm, PTFE filter media, Whatman) in falcon tubes.

2.4 Analysis

An ion chromatograph (IC; 883 basic IC plus, Metrohm, U.K.) equipped with a compact autosampler (863 Compact IC, Metrohm USA), anion column (Metrosep A Supp 4-250/4.0), and cation column (Metrosep C4-150/4.0) was used to analyze the filtered samples for concentrations of nitrate, nitrite, and ammonium, respectively (Hamid *et al.* 2015).

The removal of nitrate ($R_{NO_3^-}$) and selectivity of by-products ($S_{by-product}$) were determined on mass balance basis as given below (Hamid *et al.* 2015, Jung *et al.* 2012, 2014).

$$R_{NO_3^-} \ (\%) = \frac{[NO_3^- - N]_i - [NO_3^- - N]_f}{[NO_3^- - N]} \tag{1}$$

$$S_{NO_2^-} \ (\%) = \frac{[NO_2^- - N]_f}{[NO_3^- - N]_i - [NO_3^- - N]_f} \tag{2}$$

$$S_{NH_3^+} \ (\%) = \frac{[NH_3^- - N]_f}{[NO_3^- - N]_i - [NO_3^- - N]_f} \tag{3}$$

$$S_{N_2^-} \ (\%) = \frac{[NO_3^- - N]_i - [NO_3^- - N]_f \ - [NO_2^- - N]_f - \left[NH_4^+ - N\right]_f}{[NO_3^- - N]_i - [NO_3^- - N]_f} \tag{4}$$

Where, initial and final concentrations are denoted by subscripts *i* and *f*, respectively. Specific nitrate loading (mg NO_3-N/g catalyst/h) was calculated by following equations (Hamid *et al.* 20015, Li *et al.* 2014, Kim *et al.* 2012, Lee *et al.* 2000).

$$\text{Specific nitrate input } = \frac{QC_{NO3}}{VC_{catalyst}} \tag{5}$$

$$\text{Specific nitrate input } = \frac{C_{NO3}}{HC_{catalyst}} \tag{6}$$

Where *Q*: volumetric flow rate (L/h); C_{NO3}: nitrate concentration (mg/L) in influent; *V*: volume of reactor (L); H: HRT (h) equal to *V/Q* and $C_{catalyst}$: catalyst concentration in the reactor (g/L). Specific nitrate removal (mg NO_3-N/g catalyst/h) was determined as following

$$\text{Specific nitrate removal} = \frac{[NO_3^- - N]_i - [NO_3^- - N]_f}{HC_{catalyst}} \tag{7}$$

Cu-Pd-NZVI catalyst was identified by X-ray diffraction (XRD) (RIGAKU, D/MAX-2500, 18 KW) with Cu KN radiation. The dried samples were carefully transferred to XRD template in the anaerobic chamber after treating with 1:1 (v:v) glycerol solution to avoid the surface oxidation

(Bae and Lee 2014). Samples were scanned from 20 to 80° at a scan speed of 2θ min^{-1}. Morphological characteristics of Cu-Pd-NZVI catalyst were analyzed by transmission electron microscope/energy dispersive X-ray (TEM/EDX, Tecnai G2 F30 model, FEI company) at an acceleration voltage of 300 kV.

3. Results and discussions

3.1 Characterization

XRD analysis was performed to determine the mineral phases of Fe, Cu and Pd on fresh Cu-Pd-NZVI catalyst and the results are presented in Fig. 1. The narrow scan of newly synthesized Cu-Pd-NZVI catalyst show a well–ordered visible peak of Fe^{0} and relatively small peaks of Fe^{2+} on fresh catalyst's surface, showing that NZVI support was successfully synthesized and maintained in Fe^{0} form during catalyst preparation. The presence of Fe^{2+} could be due to oxidation of NZVI by atmospheric oxygen during sample handling. Cu and Pd peaks were not visible, perhaps due to their lower contents in catalyst composition as compared to NZVI (Jung *et al*. 2012).

TEM analysis was performed to evaluate the morphological characteristics of fresh Cu-Pd-NZVI catalyst (Fig. 2). TEM images (Fig. 2(a)) show that the spherical shaped NZVI particles (size ~50 nm) were present and cross-linked into chain-like aggregates. These particular chain-like aggregates arise from magnetic and vander Walls forces between individual NZVI particles. In addition, finely distributed particles (~5 nm) were visible on NZVI particles. EDX analysis revealed that these particles were Cu and Pd (Fig. 2(b)), indicating that Cu and Pd were present on NZVI surface and Cu-Pd-NZVI catalyst was successfully developed. Characterization results of freshly synthesized Cu-Pd-NZVI catalyst by XRD and TEM/EDX show that catalyst contains Fe^{0}, Cu and Pd according to synthesis plan.
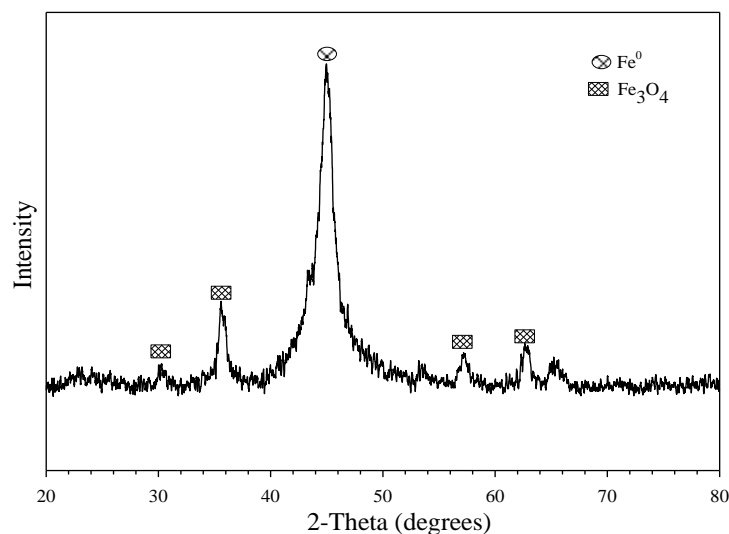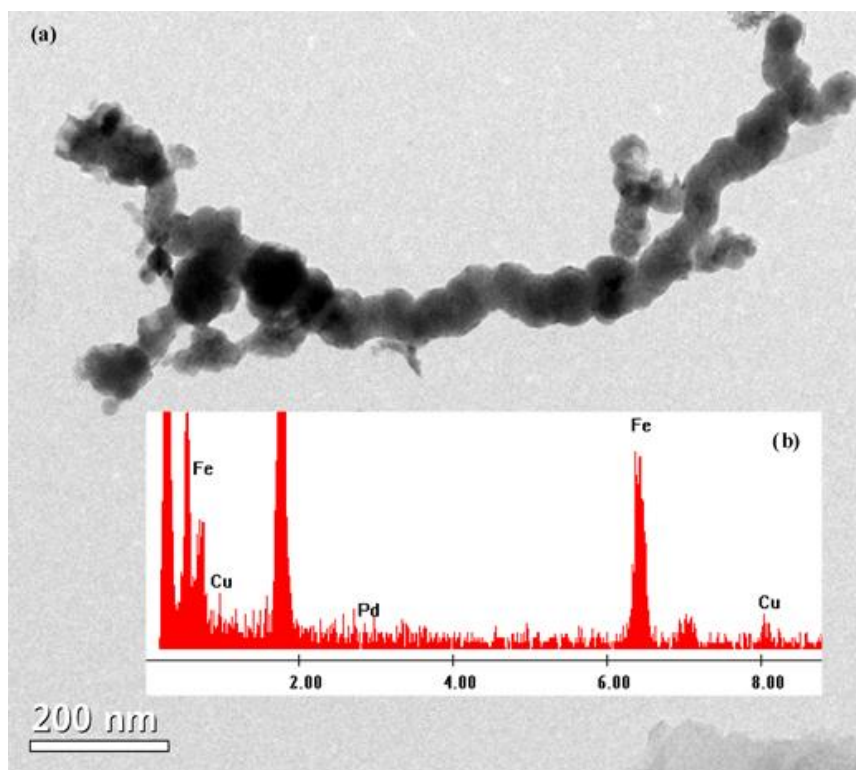

Fig. 1 XRD of fresh Cu-Pd- NZVI catalyst

Fig. 2 TEM micrographs (a) and EDX spectra; (b) of fresh Cu-Pd-NZVI catalyst

3.2 Effect of NO_3^- loading on its removal and by product selectivity

Fig. 3 shows NO_3^- removal and byproduct production profiles at four different NO_3^- loading (10, 30, 150 and 300 mg/L NO_3^--N). The other conditions were set as following: catalyst loading: 2 g/L; hydraulic retention time (HRT): 60 min; H_2 supply: 30 mL/min; and mixing speed: 300 rpm. A 100% NO_3^- was successfully removed for 9 h at 10 and 30 mg/L NO_3^--N loadings. However, NO_3^- removal significantly dropped for 150 and 300 mg/L NO_3^--N (Fig. 3(a)). NH_4^+ production decreased (Fig. 3(b)), while NO_2^- production increased (Fig. 3(c)) when NO_3^- loading increased from 10 to 300 mg/L NO_3^--N. These trends originate form change in equation of active catalyst phase and target pollutant (NO_3^-). At fixed HRT, the time to contact and react on catalyst surface is fixed to a specific amount of nitrate (Hamid *et al*. 2015). The increase in NO_3^- loading could enhance the adsorption/reduction of NO_3^- on the catalyst surface by a limited NO_3^- concentration. However, very high concentrations of NO_3^- (e.g., 150 and 300 mg/L NO_3^--N) could saturate the catalyst surface and then repel the remnant NO_3^- in aqueous phase. Thus the remnant excess amount of NO_3^- could have been washed out of the reactor without any contact with the active phase of catalyst and ultimately the overall removal efficiency declined. To verify this hypothesis, "specific NO_3^- input" and "specific NO_3^- removal" were calculated (Hamid *et al*. 2015) as described by equations 5-7, and the results are presented in Fig. 4 along with NO_3^- removal and byproduct selectivity. Fig. 4 shows that the specific NO_3^- input increased from 5 mg NO_3^--N/$g_{catalyst}$/h to 150 mg NO_3^--N/$g_{catalyst}$/h when NO_3^- loading increased from 10 to 300 mg/L, respectively.

However, the data analysis of NO_3^- reduction on Cu-Pd-NZVI catalyst show that the specific NO_3^- removal was ~37 mg NO_3^--N/$g_{catalyst}$/h. It is obvious from the results that all influent NO_3^- less than or equal to 37 mg NO_3^--N/$g_{catalyst}$/h was successfully removed, while NO_3^- in access over this specific loading was washed out of the reactor without being treated or even without any contact to the reactive surface. Fig. 4 also shows that NH_4^+ selectivity decreased and NO_2^- selectivity increased, while N_2 selectivity showed a volcanic shape with the increase in NO_3^- loading. The increase in NO_2^- selectivity shows that NO_3^- to NO_2^- reduction on Cu was not disturbed. However, the decrease in NH_4^+ selectivity could be due to 1) loss of NO_3^- reduction to NH_4^+ on NZVI due to oxidation of Fe^0 to Fe^{2+}; and 2) loss of NO_2^- reduction to NH_4^+ on Pd surface due to adsorption of excessive amount of nitrite. The excessive NO_2^- adsorption on Pd surface created net negative charge on solid surface thus repelling further NO_2^- adsorption/reduction due to columbic repulsion. Due to this reason, eventually the NH_4^+ production was suppressed while NO_2^- production was favored (Hamid *et al.* 2015). The results from this study suggest that a proper balance between active phase and pollutant should be maintained in order to achieve expected concentrations of pollutant and byproducts in effluent. The results also show that byproduct concentrations should also be carefully monitored depending on any changes in the influent target concentration.
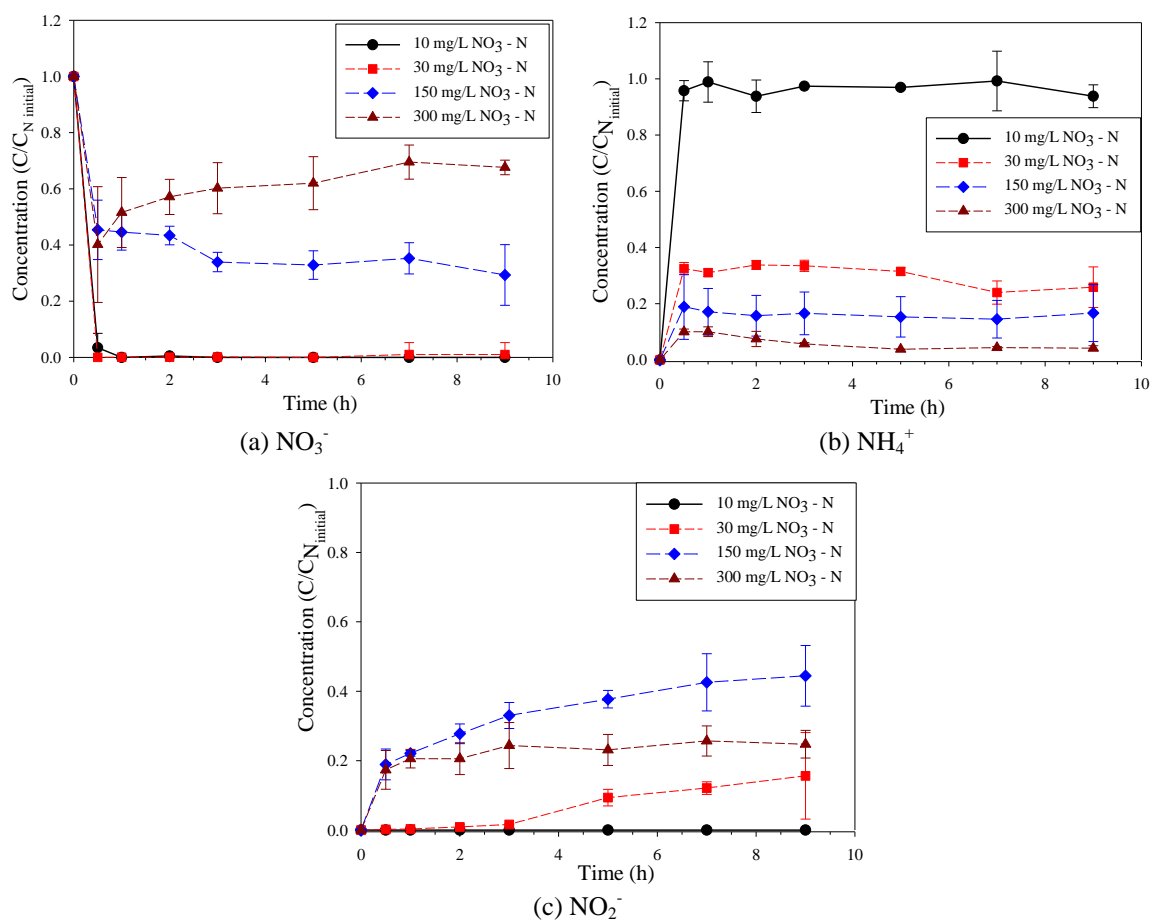

(a) NO_3^-

(b) NH_4^+

(c) NO_2^-

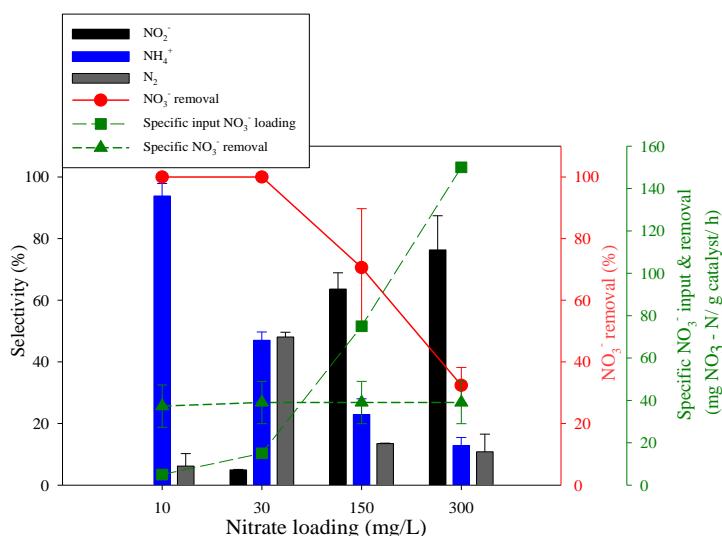Fig. 3 NO_3^- removal (a) and byproducts profiles (b-c) for various NO_3^- concentrations

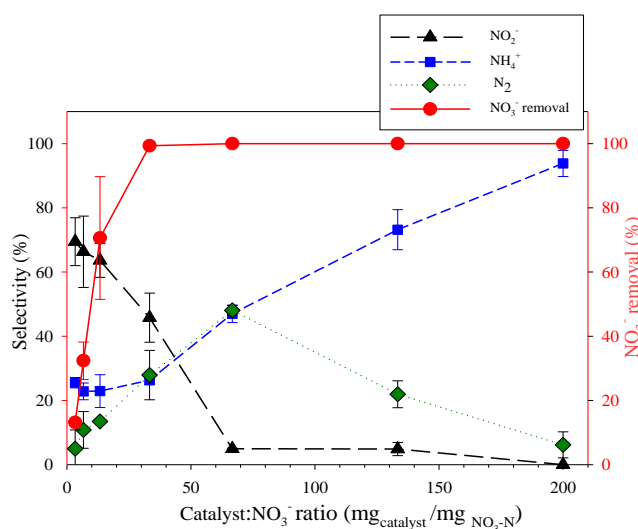Fig. 4 NO_3^- removal and byproducts selectivity at different NO_3^-

Fig. 5 NO_3^- removal and byproducts profiles at different catalyst: NO_3^- ratio

3.3 Effect of variation in catalyst to nitrate ratios

The results from NO_3^- loading experiments in previous section suggest that the nitrate removal in Cu-Pd-NZVI bimetallic system could be improved by improving catalyst ratios. Hence, more experiments were performed to evaluate the effect of catalyst to NO_3^- ratio on its removal. The results are presented in Fig. 5 which shows that NO_3^- removal efficiency enhanced from 25% to 100% when catalyst to NO_3^- ratio increased from 3.3 to $\geq$ 33 mg$_{catalyst}$/mg$_{NO3-N}$, showing that a certain minimum balance is necessary to achieve complete reduction. The NO_2^- selectivity decreased, while NH_4^+ selectivity increased with the increase in catalyst to NO_3 ratio, which is in

accordance to the expected results described in the previous section. The N_2 selectivity showed a volcanic shape and maximum N_2 selectivity (47%) was observed at ratio of 66. The results from this experiment confirm the necessity of proper optimization and monitoring for the development of catalytic nitrate reduction technology for field-scale applications.

4. Conclusions

NZVI based remediation technology is an established and effective alternative for diverse soil and groundwater pollution problems. In this study, nitrate reduction by bimetallic Cu-Pd-NZVI catalyst was evaluated under different nitrate concentration regimes in a continuous system. Results obtain in this study indicate that NO_3^- removal and byproduct selectivity by Cu-Pd-NZVI catalyst is strongly affected by influent NO_3^- concentrations and catalyst to NO_3^- ratios. Complete NO_3^- removal and high N_2 selectivity could be achieved at ≤ 37 mg NO_3-N/ g catalyst /h showing that the optimized system can take the shock loading by a certain upper limit. The results also highlight that the byproduct selectivity in a catalytic nitrate reduction process is sensitive to changes in the regimes beyond certain optimized parameters. This study concludes that change in influent target concentrations should be carefully maintained by adjusting optimum ratios and the changes should be closely monitored for a safe and efficient system. The results from this study can enhance the fundamental understanding of catalytic system dynamics and help provide novel solutions to global nitrate pollution issue.

Acknowledgments

References

Al Bahri, M., Calvo, L., Gilarranz, M.A., Rodriguez, J.J. and Epron, F. (2013), "Activated carbon supported metal catalysts for reduction of nitrate in water with high selectivity towards N_2", *Appl. Catal. B-Environ.*, **138**, 141-148.

Bae, S. and Lee, W. (2014), "Influence of riboflavin on nanoscale zero-valent iron reactivity during the degradation of carbon tetrachloride", *Environ. Sci. Technol.*, **48**(4), 2368-2378.

Bae, S., Jung, J. and Lee, W. (2013), "The effect of pH and zwitterionic buffers on catalytic nitrate reduction by TiO_2 bimetallic catalyst", *Chem. Eng. J.*, **232**, 327-337.

Choi, J., Batchelor, B., Won, C. and Chung, J. (2012), "Nitrate reduction by green rusts modified with trace metals", *Chemosphere*, **86**(8), 860-865.

Hamid, S., Bae, S., Lee, W., Amin, M.T. and Alazba, A.A. (2015), "Catalytic nitrate removal in continuous bimetallic Cu-Pd/NZVI system", *Ind. Eng. Chem. Res.*, **54**(24), 6247-6257.

Jung, J., Bae, S. and Lee, W. (2012), "Nitrate reduction by maghemite supported Cu-Pd bimetallic catalyst", *Appl. Catal. B-Environ.*, **127**, 148-158.

Jung, S., Bae, S. and Lee, W. (2014), "Development of Pd−Cu/Hematite catalyst for selective nitrate reduction", *Environ. Sci. Technol.*, **48**(16), 9651-9658.

Kim, H., Kim, T., Ahn, V., Hwang, K., Park, J., Lim, T. and Hwang, I. (2012), "Aging characteristics and reactivity of two types of nanoscale zerovalent iron particles (FeBH and FeH_2) in nitrate reduction", *Chem. Eng. J.*, **197**, 16-23.

Lee, W., Batchelor, B. and Schlautman, M.A. (2000), "Reductive capacity of soils for chromium", *Environ. Technol.*, **21**(8), 953-963.

Li, S., Wang, W., Yan, W. and Zhang, W. (2014), "Nanoscale zero-valent iron (nZVI) for the treatment of concentrated Cu(II) wastewater: a field demonstration", *Environ. Sci.: Processes Impacts*, **16**(3), 524-533.

Liou, Y.H., Lin, C.J., Weng, S.C., Ou, H.H. and Lo, S.L. (2009), "Selective decomposition of aqueous nitrate into nitrogen using iron deposited bimetals", *Environ. Sci. Technol.*, **43**(7), 2482-2488.

Liu, H., Guo, M. and Zhan, Y. (2014), "Nitrate removal by Fe^0/Pd/Cu nanocomposite in Groundwater", *Environ. Technol.*, **35**(7), 917-924.

Pintar, A. (2003), "Catalytic processes for the purification of drinking water and industrial effluents", *Catal. Today*, **77**(4), 451-465.

Pirkanniemi, K. and Sillanpaab, M. (2002), "Heterogeneous water phase catalysis as an environmental application: a review", *Chemosphere*, **48**(10), 1047-1060.

Shin, H., Jung, S., Bae, S., Lee, W. and Kim, H. (2014), "Nitrite reduction mechanism on a Pd surface", *Environ. Sci. Technol.*, **48**(21), 12768-12774.

Soares, O.S.G.P., Órfa, J.J.M., Gallegos-Suarez, E., Castillejos, E., Rodríguez-Ramos, I. and Pereira, M.F.R. (2012), "Nitrate reduction over a PdCu/MWCNT catalyst: application to a polluted groundwater", *Environ. Technol.*, **33**(20), 2353-2358.

WL